A Novel Nonlinear Backstepping Controller Design for Helicopters Using the Rotation Matrix

Ioannis A. Raptis, Kimon P. Valavanis, *Senior Member, IEEE*, and Wilfrido A. Moreno, *Member, IEEE*

***Abstract*—This brief presents a backstepping controller design for helicopters. The controller objective is for the helicopter to autonomously track predefined position and yaw reference trajectories. The incorporation of nested saturation feedback functions in the backstepping design preserves the helicopter's motion and power physical constraints. The intermediate control signals related to the attitude dynamics exploit the structural properties of the rotation matrix and are enhanced with terms that guarantee that the helicopter will not overturn while tracking the desired position trajectory. The attitude dynamics are rendered exponentially stable while the translational dynamics are globally asymptotically stable. Numerical simulations illustrate the applicability of the proposed design.**

***Index Terms*—Attitude control, backstepping control, bounded control, helicopter control, nonlinear control.**

I. Introduction

HELICOPTERS are highly nonlinear systems with significant dynamic coupling. This dynamic coupling is attributed to the force and torque generation process. There is also significant parameter and model uncertainty due to the complicated aerodynamic nature of the thrust generation. Therefore, there is a major interest in theoretical perspectives of helicopter controller designs and their implementation to autonomous flight.

In general, most control designs are based on linearized helicopter dynamics using the widely adopted concept of stability derivatives [2]–[4]. However, in recent years there is considerable research related to helicopter flight control based on nonlinear dynamic representations [5]–[10].

This brief presents a novel nonlinear controller design for helicopters. The main objective is for the helicopter to track a predefined, possibly aggressive, position and yaw reference trajectories with certain bounds that reflect the helicopter's physical limitations. The controller is based on the backstepping design principle for systems in feedback form. The intermediate backstepping control signals (a.k.a. pseudo controls) for each level of the feedback system are appropriately chosen to stabilize the overall helicopter dynamics.

The pseudo control choice for the translational dynamics subsystem involves the use of a nested saturation feedback signal of the translational position and velocity error. The pseudo controls associated with the attitude dynamics use the structural properties of the rotation matrix and guarantee that the orientation error is rendered exponentially stable. The exponential stability of the orientation error will result in the asymptotic tracking of the desired position trajectory.

One of the novelties of the proposed controller, is that apart from stabilizing the attitude dynamics, the control design can guarantee that the helicopter will not overturn for every allowed reference trajectory. In addition, the thrust magnitude is used to compensate the translational error dynamics in all Cartesian directions and not only for the heave dynamics. The use of nested saturations in the intermediate pseudo controls of the translational dynamics can guarantee that the physical constraints of the helicopter motion and power will be preserved.

This brief is organized as follows. In Section II, the helicopter model is introduced. The translational error dynamics and the attitude error dynamics are presented in Sections III and IV, respectively. The stability analysis of the attitude error dynamics is presented in Section V, while the stability analysis of the translational error dynamics is presented in Section VI. Finally, simulation results and conclusions are given in Sections VII and Section VIII, respectively.

II. Helicopter Model

Mathematical Notation

The abbreviations C_t and S_t with $t \in \mathbb{R}$ represent the trigonometric functions $\cos(t)$ and $\sin(t)$, respectively. The superscript T indicates the transpose of a vector or matrix. The operands $\|(\cdot)\|$, $|(\cdot)|$ denote the Euclidean norm and the $\|(\cdot)\|_1$ norm of a vector, respectively. For a vector $\vec{w} \in \mathbb{R}^3$ the notation $\hat{\vec{w}}$ denotes the skew symmetric matrix of $\mathbb{R}^{3\times 3}$.

A. Rigid Body Dynamics

The analysis and most of the notation in Section II follows [5] and [7]. The first step towards the development of the rigid body's equations of motion is the definition of two reference frames. Each frame is fully characterized by its center and three mutually orthonormal vectors. The first one is the inertia frame defined as $\mathcal{F}_I = \{O_I, \vec{i}_I, \vec{j}_I, \vec{k}_I\}$. The second is the body fixed reference frame defined as $\mathcal{F}_B = \{O_B, \vec{i}_B, \vec{j}_B, \vec{k}_B\}$, where the center O_B is located at the center of gravity (CG) of the helicopter. The direction of the body fixed frame orthonormal vectors $\{\vec{i}_B, \vec{j}_B, \vec{k}_B\}$ is shown in Fig. 1.

Manuscript received July 12, 2009; revised October 22, 2009. Manuscript received in final form January 29, 2010. First published March 11, 2010; current version published February 23, 2011. Recommended by Associate Editor F. A. Cuzzola. This work was supported in part by NSF Grant, IIP-0856311 (DU Grant 36563). This brief is the extended version of a paper published in the Proceedings of the 17th Mediterranean Conference on Control Automation, pp. 1227–1232, 2009.

I. A. Raptis and W. A. Moreno are with the Department of Electrical Engineering, University of South Florida, Tampa, FL 33620 USA (e-mail: iraptis@mail.usf.edu; moreno@eng.usf.edu).

K. P. Valavanis is with the Department of Electrical and Computer Engineering, University of Denver, Denver, CO 80208 USA (e-mail: kimon.valavanis@du.edu).

Digital Object Identifier 10.1109/TCST.2010.2042450

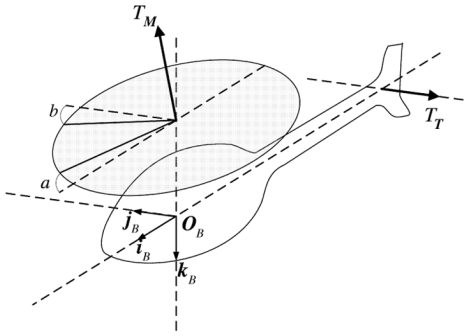

Fig. 1. Helicopter's body frame, the tip-path-plane angles, and the thrust vectors of the main and tail rotor.

Following the analysis in [5] denote $F^B = [f^B \tau^B]^T \in \mathbb{R}^6$ as the external wrench acting on the CG of the helicopter, expressed in the body frame coordinates. The rotation matrix R is parametrized with respect to the three Euler angles roll (ϕ), pitch (θ) and yaw (ψ) and maps vectors from the body fixed frame $\mathcal{F}_B$ to the inertia frame $\mathcal{F}_I$. The rotation matrix results from three consecutive rotations by the roll-pitch-yaw angles each of them taking place in the current frame. From standard results

$$R = \begin{bmatrix} C_\psi C_\theta & -S_\psi C_\phi + C_\psi S_\theta S_\phi & S_\phi S_\psi + C_\phi S_\theta C_\psi \\ S_\psi C_\theta & C_\phi C_\psi + S_\phi S_\theta S_\psi & -C_\psi S_\phi + S_\psi S_\theta C_\phi \\ -S_\theta & C_\theta S_\phi & C_\theta C_\phi \end{bmatrix}.$$

The orientation vector is given by $\Theta = [\phi\ \theta\ \psi]^T$ and from standard results the associated orientation dynamics are governed by $\dot{\Theta} = \Psi(\Theta)\omega^B$, where

$$\Psi(\Theta) = \begin{bmatrix} 1 & S_\phi S_\theta / C_\theta & C_\phi S_\theta / C_\theta \\ 0 & C_\phi & -S_\phi \\ 0 & S_\phi / C_\theta & C_\phi / C_\theta \end{bmatrix}. \quad (1)$$

The angular velocity with respect to the body frame is $\omega^B = [\omega_x\ \omega_y\ \omega_z]^T \in \mathbb{R}^3$. Let $p^I = [p_x^I\ p_y^I\ p_z^I]^T \in \mathbb{R}^3$ denote the position vector of the CG of the helicopter with respect to the inertial coordinates, and $v^I = [v_x\ v_y\ v_z]^T \in \mathbb{R}^3$ denote the linear velocity vector in inertial coordinates. The complete dynamic equations of the rigid body in the configuration space $SE(3) = \mathbb{R}^3 \times SO(3)$ are

$$\dot{p}^I = v^I \quad (2)$$
$$\dot{v}^I = \frac{1}{m} R f^B \quad (3)$$
$$\dot{R} = R\hat{\omega}^B \quad (4)$$
$$\mathcal{I}\dot{\omega}^B = -\omega^B \times (\mathcal{I}\omega^B) + \tau^B \quad (5)$$

where $\mathcal{I}$ denotes the inertia matrix of the helicopter with respect to the body fixed reference frame. The helicopter's rigid body dynamics given in (2)–(5) will be completed by defining the external body frame force f^B and torque τ^B.

B. External Wrench Model

In this brief, the modeling approach of [5], [11], [12] is followed, which provides a simplified external wrench model adequate for control design purposes. The thrust vector produced by the main rotor is considered perpendicular to the tip-path-plane (TPP). The TPP is the plane where the tips of the blades lie and it is used to provide a simplified representation of all the rotors blades [12].

There are four control inputs associated with helicopter piloting. The control input vector is defined as $u = [T_M\ T_T\ a\ b]^T$. The components T_M and T_T are the magnitudes of the generated thrusts by the main and tail rotor, respectively. The other two control commands are the flapping angles a, b and they represent the tilt of the TPP at the longitudinal and lateral axis, respectively. The positive direction of the flapping angles is also depicted in Fig. 1.

Let $\vec{T}_M$ and $\vec{T}_T$ denote the thrust vector of the main and tail rotor, respectively. By simple geometry the following equations are derived:

$$\vec{T}_M = \begin{bmatrix} X_M \\ Y_M \\ Z_M \end{bmatrix} = \begin{bmatrix} -S_a C_b \\ C_a S_b \\ -C_a C_b \end{bmatrix} T_M \approx \begin{bmatrix} -a \\ b \\ -1 \end{bmatrix} T_M. \quad (6)$$

The above equation is simplified by assuming small angle approximation ($\cos(\cdot) \approx 1$ and $\sin(\cdot) \approx (\cdot)$) for the flapping angles. The small angle assumption is adopted by [5], [12], [13]. For the tail rotor

$$\vec{T}_T = [0 \quad Y_T \quad 0]^T = [0 \quad -1 \quad 0]^T T_T. \quad (7)$$

Therefore, by including the helicopter's weight, the complete force vector will be

$$f^B = \begin{bmatrix} X_M \\ Y_M + Y_T \\ Z_M \end{bmatrix} + R^T \begin{bmatrix} 0 \\ 0 \\ mg \end{bmatrix}. \quad (8)$$

A common simplification practice followed in [5], [7], and [8] is to neglect the effect of the lateral and longitudinal forces produced by the TPP tilt and the effect of the tail rotor thrust. Those parasitic forces have a minimal effect on the translational dynamics compared to the Z_M component. In this case, the only two forces applied to the helicopter are the main rotor's thrust vector at the direction of $\vec{k}_B$ of the body frame and the weight force. Therefore, (8) becomes

$$f^B = [0 \quad 0 \quad -T_M]^T + R^T [0 \quad 0 \quad mg]^T. \quad (9)$$

The generated torques are the result of the above forces and the rotors moments. Denote $\vec{h}_M = [x_m\ y_m\ z_m]^T$ and $\vec{h}_T = [x_t\ y_t\ z_t]^T$ as the position vectors of the main and tail rotor shafts, respectively (expressed in the body coordinate frame). Let $\tau_M^B = \vec{h}_M \times \vec{T}_M$ and $\tau_T^B = \vec{h}_T \times \vec{T}_T$ be the torques generated by $\vec{T}_M$ and $\vec{T}_T$, respectively. The complete torque vector will be

$$\tau^B = \tau_M + \tau_M^B + \tau_T^B \quad (10)$$

with $\tau_M = [R_M\ M_M\ N_M]^T$ and

$$R_M = c_m b - Q_M S_a C_b$$
$$M_M = c_m a + Q_M S_b C_a$$
$$N_M = -Q_M C_a C_b$$
$$Q_M = C^M T_M^{1.5} + D^M$$

where c_m is a positive constant associated with the main rotor's stiffness and Q_M is the main rotor's anti-torque. The positive constants C^M and D^M are associated with the generation of the reaction torque Q_M. A detailed description of τ_M can be found in [5] and [14]. Substituting (6), (7)–(10) a more compact form of the torque can be given as

$$\tau^B = A(T_M)v_c + B(T_M) \tag{11}$$

where $v_c = (a\ b\ T_T)^T$, with $A(T_M) \in \mathbb{R}^{3\times 3}$ being an invertible matrix for bounded T_M and $B(T_M) \in \mathbb{R}^{3\times 1}$.

C. Complete Rigid Body Dynamics

Using the force simplification assumption given in (9) and the applied torque given by (11), the translational and angular velocity helicopter dynamics are expressed as

$$\dot{v}^I = -\frac{1}{m}Re_3T_M + ge_3 \tag{12}$$

$$\mathcal{I}\dot{\omega}^B = -\omega^B \times (\mathcal{I}\omega^B) + A(T_M)v_c + B(T_M) \tag{13}$$

where $e_3 = [0\ 0\ 1]^T$. The proposed controller applies backstepping design principles, which are ideal for systems of feedback form.

III. Translational Error Dynamics

Consider a helicopter described by the dynamic equations (2), (4) and (12), (13). The objective is to design a controller regulating position p^I and the yaw angle ψ to the desired reference values $p_d^I = [p_{d,x}^I\ p_{d,y}^I\ p_{d,z}^I]^T$ and ψ_d, respectively. The proposed controller design requires that the components of p_d^I and their higher time derivatives are bounded.

Let $R = [\rho_1\ \rho_2\ \rho_3]$, where ρ_i with $i = 1, 2, 3$ are the column vectors of the rotation matrix. Denote $\rho_{i,j}$ the element of the j_{th} row and i_{th} column of the rotation matrix. Let e_ρ denote the orientation error between the actual direction of the thrust vector ρ_3, minus a desired direction denoted by $\rho_d = [\rho_{d,1}\ \rho_{d,2}\ \rho_{d,3}]^T$. Following standard procedure of the backstepping design, the translational error dynamics of the helicopter can be written as

$$\dot{e}_p = \dot{p}^I - \dot{p}_d^I = e_v$$
$$\dot{e}_v = \dot{v}^I - \dot{v}_d^I = ge_3 - \ddot{p}_d^I - \frac{1}{m}\rho_d T_M - \frac{1}{m}e_\rho T_M.$$

The elements of the unitary vector ρ_3 express the inertia coordinates of the body's frame vector $\vec{k}_B$. The term $-\rho_3 T_M$ represents the helicopter's thrust force. The main design idea of this step is to choose the desired direction and magnitude of the thrust vector (ρ_d and T_M, respectively) in such a way so that the translational error dynamics will be globally asymptotically stable (GAS) by disregarding initially the effect of e_ρ. As it will be illustrated, the proposed choice of ρ_d and T_M followed by the exponential stability of the orientation error e_ρ, will guarantee that the complete translational error dynamics will be uniformly globally asymptotically stable (UGAS) for any initial condition of the position and translational velocity.

The following desired values will be chosen:

$$\rho_d = \frac{-\ddot{p}_d^I + ge_3 + \Sigma_2(e_v + \Sigma_1(W(e_v + e_p)))}{\| -\ddot{p}_d^I + ge_3 + \Sigma_2(e_v + \Sigma_1(W(e_v + e_p)))\|} \tag{14}$$

$$T_M = m\| -\ddot{p}_d^I + ge_3 + \Sigma_2(e_v + \Sigma_1(W(e_v + e_p)))\| \tag{15}$$

where $W = \text{diag}(w_1, w_2, w_3)$ with $w_i > 0$ for $i = 1, 2, 3$ and

$$S(e_p, e_v) = \Sigma_2(e_v + \Sigma_1(W(e_v + e_p))) \tag{16}$$

with $\Sigma_i(x) = [\sigma_{i,1}(x_1)\ \sigma_{i,2}(x_2)\ \sigma_{i,3}(x_3)]^T$ for $i = 1, 2$ and $x = [x_1\ x_2\ x_3]^T$. The function σ denotes a saturation function, which is defined as follows.

Definition 1: The function $\sigma : \mathbb{R} \to \mathbb{R}$ is a continuous, twice differentiable, nondecreasing function for which given two positive numbers L, M with $L \leq M$ the following properties hold:

- P.1) $\sigma(s) = s$ when $|s| \leq L$;
- P.2) $|\sigma(s)| \leq M$ for every $s \in \mathbb{R}$;
- P.3) $s\sigma(s) > 0$ for every $s \neq 0$;
- P.4) $|\sigma(s)| \leq |s|$ for every $s \in \mathbb{R}$;
- P.5) $\sigma(s)$ is globally Lipschitz in s.

The above definition of the linear saturation function is similar to the definition given in [15]. Two additional properties are added. The twice differentiability and the globally Lipschitz property (P.5), which are necessary for the backstepping design.

From (14) it is obvious that ρ_d is chosen to be a unitary vector. Furthermore, the helicopter during the flight operation is required not to overturn while tracking the reference maneuver. More specifically it is required that $|\phi(t)| < \pi/2$ and $|\theta(t)| < \pi/2$ for every $t \geq t_0$. Apart from the physical helicopter flight limitations, this condition is necessary to avoid singularities in the rotation matrix representation by the Euler angles. Similar constraints apply by the use of quaternions for the attitude representation [7], [16]. When the helicopter is tracking its desired orientation, dictated by the directional vector ρ_d, the same limitation should apply. In other words, $|\phi_d(t)| < \pi/2$ and $|\theta_d(t)| < \pi/2$ for every $t \geq t_0$. From (14), an additional constraint is imposed on the choice of the saturation vector $S(e_p, e_v)$ and the desired position trajectory. This constraint is sufficient to guarantee that $\rho_{d,3} = C_{\theta_d}C_{\phi_d} > 0$ for every $t \geq t_0$.

Property 1: If for every $t \geq t_0$ the saturation level $M_{2,3}$ of the function $\sigma_{2,3}$ and the predefined value of $\ddot{p}_{d,z}^I$ satisfy the inequality

$$g - M_{2,3} > \max_{t \geq t_0} \ddot{p}_{d,z}^I(t)$$

then $\rho_{d,3}(t) > 0$ and consequently $|\phi_d(t)|, |\theta_d(t)| < \pi/2$ for every $t \geq t_0$.

Substitution of the desired values given in (14)–(15) will result in the following representation of the translational error dynamics:

$$\dot{e}_p = e_v$$
$$\dot{e}_v = -S(e_p, e_v) - \underbrace{(\rho_3(\Theta) - \rho_d(t))}_{e_\rho} U(t, e_p, e_v)$$

where

$$U(t, e_p, e_v) = \| -\ddot{p}_d^I + ge_3 + \Sigma_2(e_v + \Sigma_1(W(e_v + e_p)))\|.$$

The translational error dynamics subsystem can be considered as a GAS nominal system of a single integrator controlled

by a nested saturation feedback law. The nominal system is perturbed by a bounded term of the orientation error e_ρ. The stability analysis of the resulting translational error dynamics will be investigated in detail in Section VI.

Before we proceed with the analysis of the attitude dynamics subsystem, the following observation is mentioned. Since ρ_3 and ρ_d are unitary vectors there is an additional constraint expressed by the equality $\rho_{3,3} = \sqrt{1-\rho_{3,1}^2-\rho_{3,2}^2}$ given that $\rho_{3,3} \geq 0$. Due to this constraint it is shown that only exponential decay of the vector $e_r = r - r_d$ with $r = [\rho_{3,1}\ \rho_{3,2}]^T$ and $r_d = [\rho_{d,1}\ \rho_{d,2}]^T$ is required. The vectors r and r_d lie in the x–y plane of the inertia frame. Given that the controller design guarantees that the helicopter will not overturn ($\rho_{3,3}(t) > 0$ for every $t > t_0$) the exponential convergence of $\rho_{3,3}$ to $\rho_{d,3}$ follows.

Definition 2: Denote the following open and connected sets:
1) $\mathcal{P} = (0 \quad 1]$;
2) 2-D set $\mathcal{Q} = \{v \in \mathbb{R}^2 : \|v\| < 1\}$;
3) 2-D set $\mathcal{E} = (-2 \quad 2) \times (-2 \quad 2)$.

Consequence of the angle bounds $|\theta|, |\phi| < \pi/2$ and $|\theta_d|, |\phi_d| < \pi/2$ are the statements of the following Proposition.

Proposition 1: When $\rho_{3,3}, \rho_{d,3} \in \mathcal{P}$ then we have the following:
1) $|\phi|, |\phi_d|, |\theta|, |\theta_d| < \pi/2$;
2) $r, r_d \in \mathcal{Q}$;
3) $e_r \in \mathcal{E}$.

IV. Attitude Error Dynamics

This section presents the attitude error dynamics subsystem. Apart from the stabilization part, additional goal for the control law is to keep $|\theta(t)|, |\phi(t)| < \pi/2$ for every $t \geq t_0$ and for any initial condition of the attitude dynamics for which the helicopter is not overturned.

A. Yaw Error Dynamics

Let $e_\psi = \psi - \psi_d$ be the error of the yaw angle, then the error dynamics will be

$$\dot{e}_\psi = -\dot{\psi}_d + \frac{S_\phi}{C_\theta}\omega_y + \frac{C_\phi}{C_\theta}\omega_z.$$

Using ω_z as the pseudo control, the error dynamics for the yaw angle can be written as

$$\dot{e}_\psi = -\dot{\psi}_d + \frac{S_\phi}{C_\theta}\omega_y + \frac{C_\phi}{C_\theta}\omega_{z,d} + \alpha(\phi,\theta)e_\omega$$

where $e_\omega = \omega^B - \omega_d^B$, with $\omega_d^B = [\omega_{x,d}\ \omega_{y,d}\ \omega_{z,d}]^T$ and $\alpha(\phi,\theta) = [0\,0\,(C_\phi)/(C_\theta)]$. The value of $\omega_{z,d}$ will be chosen in such a way to cancel out the nonlinear terms and stabilize the yaw error dynamics. The choice is

$$\omega_{z,d} = \frac{C_\theta}{C_\phi}\left[\dot{\psi}_d - \frac{S_\phi}{C_\theta}\omega_y - \lambda_\psi e_\psi\right] \tag{17}$$

where λ_ψ is a positive gain.

B. Orientation Error Dynamics

As mentioned earlier due to the constraint of orthonormality of the vector ρ_3 the orientation analysis can be restricted to the vector $r \in \mathcal{E}$. As it will be shown, exponential stabilization of the error dynamics $e_r = r - r_d$ will guarantee the exponential stabilization of e_ρ. The reduced orientation error dynamics are

$$\dot{e}_r = -\dot{r}_d + Z(\Theta)\begin{bmatrix}\omega_{x,d}\\ \omega_{y,d}\end{bmatrix} + Z(\Theta)\begin{bmatrix}e_{\omega,x}\\ e_{\omega,y}\end{bmatrix}$$

where

$$Z(\Theta) = \begin{bmatrix}-\rho_{2,1} & \rho_{1,1}\\ -\rho_{2,2} & \rho_{1,2}\end{bmatrix}$$

$$\text{with } Z^{-1}(\Theta) = \frac{1}{\rho_{3,3}}\begin{bmatrix}\rho_{1,2} & -\rho_{1,1}\\ \rho_{2,2} & -\rho_{2,1}\end{bmatrix}.$$ [1]

The choice of the angular velocity pseudo controls is

$$\begin{bmatrix}\omega_{x,d}\\ \omega_{y,d}\end{bmatrix} = Z^{-1}(\Theta)\left(\dot{r}_d - \Lambda_1 e_r - \frac{k}{\rho_{3,3}}e_r\right) \tag{18}$$

where $\Lambda_1 = \mathrm{diag}(\lambda_{1,1}, \lambda_{1,2})$ with $\lambda_{1,i}, k > 0$ for $i = 1, 2$.

C. Angular Velocity Error Dynamics

The angular velocity error dynamics e_ω based on (13) have the following form:

$$\mathcal{I}\dot{e}_\omega = -\mathcal{I}\dot{\omega}_d^B - \hat{e}_\omega\mathcal{I}\omega^B - \hat{\omega}_d^B\mathcal{I}\omega^B + A(T_M)v_c + B(T_M).$$

The initial objective of v_c is to remove the effect of $A(T_M)$ and $B(T_M)$. Therefore the initial choice of v_c is

$$v_c = A^{-1}(T_M)[-B(T_M) + \tilde{v}]. \tag{19}$$

The vector $\tilde{v}$ is an additional stabilizing term of the following form:

$$\tilde{v} = \mathcal{I}\dot{\omega}_d^B + \hat{\omega}_d^B\mathcal{I}\omega^B - e_\psi\alpha(\phi,\theta)^T - \Lambda_2 e_\omega \tag{20}$$

where $\Lambda_2 \in \mathbb{R}^{3\times 3}$ is a diagonal matrix of positive gains.

V. Stability of the Attitude Error Dynamics

Applying the control v_c of (19), (20) and the pseudo controls given in (17), (18), the error attitude dynamics become

$$\begin{aligned}\dot{e}_r &= -\Lambda_1 e_r - \frac{k}{\rho_{3,3}}e_r + Z_0(\Theta)e_\omega\\ \dot{e}_\psi &= -\lambda_\psi e_\psi + \alpha(\phi,\theta)\,e_\omega\\ \mathcal{I}\dot{e}_\omega &= -\hat{e}_\omega\mathcal{I}\omega^B - e_\psi\alpha(\phi,\theta)^T - \Lambda_2 e_\omega\end{aligned} \tag{21}$$

with $Z_0(\Theta) = [Z(\Theta)\ 0_{2\times 1}]$. The complete error vector of the attitude dynamics is given by the state vector $[e_\psi\, e_r\, e_\omega]^T \in \mathcal{Z}$, where $\mathcal{Z} = \mathbb{R} \times \mathcal{E} \times \mathbb{R}^3$. Precondition for the continuity of the right-hand side of (21) is for $\rho_{3,3}$ to belong to the set $\mathcal{P}$.

[1]Note that $\rho_{3,3} = \rho_{1,1}\rho_{2,2} - \rho_{1,2}\rho_{2,1}$.

Theorem 1: Given that $\rho_{3,3}(t)$ and the desired value of $\rho_{d,3}(t)$ belong to $\mathcal{P}$ for every $t \geq t_0$, and the choice of gains

$$\lambda_{1,1} = \kappa_1 + \theta_1^2 \quad \lambda_{1,2} = \kappa_2 + \eta_1^2$$
$$\lambda_{2,\min} = \zeta + \theta_2^2 + \eta_2^2$$

where $\lambda_{2,\min}$ is the minimum entry of the gain matrix Λ_2 and $\theta_1, \theta_2, \eta_1, \eta_2, \zeta > 0$ with $\theta_1\theta_2 \geq 1/2$, $\eta_1\eta_2 \geq 1/2$, then the error dynamics of the system described by (21) are exponentially stable for any initial condition $[e_\psi(t_0)\ e_r(t_0)\ e_\omega(t_0)] \in \mathcal{Z}$.

The Proof of Theorem 1 is given in [1]. The exponential decay of the vector e_r from Theorem 1 results in the following inequalities:

$$\|e_{\rho,1}\| \leq \|e_{\rho,1}(t_0)\| e^{-\kappa_1(t-t_0)}$$
$$\|e_{\rho,2}\| \leq \|e_{\rho,2}(t_0)\| e^{-\kappa_2(t-t_0)} \quad \forall t \geq t_0.$$

Theorem 2: For the system in (21), given a desired orientation vector $\rho_d(t)$ with the vector component $\rho_{d,3}(t) > 0$ for every $t \geq t_0$, the helicopter will not overturn, satisfying $\rho_{3,3}(t) > 0$ for every $t \geq t_0$. The latter inequality of the vector component $\rho_{3,3}$ holds for every initial state of the angular velocity and the orientation of the thrust vector, given that $\rho_{3,3}(t_0) > 0$.

The Proof of Theorem 2 is given in [17]. Due to the fact that $\rho_{3,3} = C_\theta C_\phi$, Theorem 2 implies that $|\theta(t)|, |\phi(t)| < \pi/2$ for every $t \geq t_0$ given that $|\theta(t_0)|, |\phi(t_0)| < \pi/2$.

Lemma 1: Given that the conditions of Theorem 1 are met for the system in (21), the dynamics of $e_{\rho,3}$ will exponentially decay to zero, with the bound

$$\|e_{\rho,3}\| \leq \frac{2\sqrt{2}}{c_{\min}} \|e_r(t_0)\| e^{-\kappa(t-t_0)}$$

where $\kappa = \min(\kappa_1, \kappa_2)$, and $c_{\min} = \min_{t \geq t_0} \rho_{d,3}(t)$.

The Proof of Lemma 1 is given in [1]. An immediate consequence of Theorem 1 and Lemma 1 is the following property.

Property 2: Given that Theorem 1 and Lemma 1 hold, the vector e_ρ is exponentially stable for every $e_\rho(t_0) \in \mathcal{E} \times \mathcal{P}$ with the exponentially decaying bound

$$\|e_\rho\| \leq \frac{c_{\min} + 2\sqrt{2}}{c_{\min}} \|e_\rho(t_0)\| e^{-\kappa(t-t_0)}.$$

The Proof of Property 2 is given in [17]. The useful attribute of Property 2 is the exponential decay of e_ρ, which is necessary for the stability analysis of the translational error dynamics.

VI. Stability of the Translational Error Dynamics

This section examines the stability of the translational error dynamics. The first step towards the stability analysis is to perform the following linear state transformation:

$$y = \begin{bmatrix} y_1 \\ y_2 \end{bmatrix} = \begin{bmatrix} I_{3\times3} & I_{3\times3} \\ 0 & I_{3\times3} \end{bmatrix} \begin{bmatrix} e_p \\ e_v \end{bmatrix}.$$

The state transformation above will facilitate the stability analysis of this section. The resulting form of the translational dynamics is

$$\dot{y} = f(y) + g(t,y)e_\rho = G(t, y, e_\rho) \tag{22}$$

where

$$f(y) = \begin{bmatrix} y_2 - \Sigma_2(y_2 + \Sigma_1(Wy_1)) \\ -\Sigma_2(y_2 + \Sigma_1(Wy_1)) \end{bmatrix}$$
$$g(t,y) = -\begin{bmatrix} I_{3\times3} \\ I_{3\times3} \end{bmatrix} U(t,y). \tag{23}$$

The following properties are required to prove global asymptotic stability of the system in (22).

Property 3: For the nominal system

$$\dot{y} = f(y) \tag{24}$$

with $f(y)$ defined in (23), $y = 0$ is an equilibrium point. Given that, for the saturation levels of the vector S [defined in (16)], the following inequalities hold:

1) $L_{2,i} \leq M_{2,i}$ and $L_{1,i} \leq M_{1,i}$ for $i = 1, 2, 3$;
2) $M_{1,i} < (1/3)L_{2,i}$ for $i = 1, 2, 3$.

Then, based on the findings of [15], the nominal system of (24) is GAS.

The translational dynamics subsystem can be viewed as a perturbed UGAS nominal system where the perturbation term is driven by e_ρ. According to [18], in order for the solutions of the system in (22) to be UGAS, the following sufficient conditions should hold simultaneously:

C.1) nominal system of (24) is UGAS;
C.2) integral curves of e_ρ are UGAS;
C.3) solutions of the system in (22) are uniformly globally bounded (UGB).

Conditions C.1) and C.2) are guaranteed by Properties 3 and 2, respectively. Exploiting the Lipschitz property of $G(t, y, e_\rho)$ with respect to y and the exponential decaying bound of e_ρ provided by Property 2 the following, theorem will hold.

Theorem 3: Given that Theorems 1 and 2 hold, the solutions of the system given by (22) are UGB for every time $t \geq t_0$.

The Proof of Theorem 3 is given in [17]. Based on the work of [18]–[20] the stability of the helicopter translational error dynamics is formally stated in the following theorem.

Theorem 4 [18], [19]: Given that the nominal system in (24) is UGAS (Property 3), the orientation error e_ρ is exponentially convergent (Property 2), and the solutions of (22) are UGB (Theorem 3), then the solutions of the perturbed system in (22) are UGAS.

Theorems 1, 2, and 4 guarantee that the controller design objectives are met. More specific, for any desired position reference trajectory p_d^I with bounded higher derivatives satisfying the requirements of Property 1 and for every desired yaw heading ψ_d

$$\lim_{t\to\infty} \|p^I - p_d^I\| = 0 \quad \lim_{t\to\infty} \|\psi - \psi_d\| = 0$$
$$|\theta(t)|, |\phi(t)| < \pi/2 \quad \forall t \geq t_0$$

for any initial condition $[p^I(t_0)\, v^I(t_0)\, \omega^B(t_0)\, \psi(t_0)]^T \in \mathbb{R}^{10}$ given that the helicopter is not initially overturned ($|\theta(t_0)|, |\phi(t_0)| < \pi/2$).

VII. Simulations

This section presents the numeric simulation results of the control algorithm. For the helicopter model, the complete repre-

sentation of the thrust vector is used given in (8), which includes the parasitic elements X_M, Y_M and Y_T. However, the control design was based on the simplified force vector representation of (9). Furthermore, the total body force and moment vectors of (8) and (10) are additionally perturbed by the total drag force and moment vectors f_d^B and τ_d^B, respectively. The drag forces and moments are produced by the effect of the relative wind velocity and air pressure, to the surfaces of the helicopter's fuselage, vertical fin and horizontal stabilizer. To represent the complete drag force and moment vectors we have adopted the model given in [8], which is a simplified version of the more elaborate description presented in [21]. Those vectors are

$$f_d^B = \begin{bmatrix} -d_x^f v_{a,x}^B V_\infty \\ -d_y^f v_{a,y}^B V_\infty - d_y^{vf}|v_{vf}|v_{vf} \\ -d_z^f \left(v_{a,z}^B + V_i\right) V_\infty + d_z^{hs}|v_{hs}|v_{hs} \end{bmatrix}$$

$$\tau_d^B = \begin{bmatrix} z_t d_y^{vf}|v_{vf}|v_{vf} \\ -x_{hs} d_z^{hs}|v_{hs}|v_{hs} \\ -x_t d_y^{vf}|v_{vf}|v_{vf} \end{bmatrix}$$

where $d_x^f, d_y^f, d_z^f, d_y^{vf}, d_z^{hs}$ are constant parameters that depend on the air density as well as the geometry of the fuselage, the vertical fin and horizontal stabilizer. The constant V_i denotes the main rotor's induced velocity while x_{hs} is the coordinate of the horizontal stabilizer in the $\vec{i}_B$ direction of the body frame. The relative wind velocity vector $v_a^B = [v_{a,x}^B\ v_{a,y}^B\ v_{a,z}^B]^T$ is given by $v_a^B = v^B - v_w^B$, where v_w^B denotes the wind velocity in the body frame coordinates. The rest of the velocity components involved in the drag force and moment model, are

$$v_{vf} = v_{a,y}^B + x_t\omega_z \quad v_{hs} = v_{a,z}^B - x_{hs}\omega_y$$
$$V_\infty = \sqrt{\left(v_{a,x}^B\right)^2 + \left(v_{a,y}^B\right)^2 + \left(v_{a,z}^B + V_i\right)^2}.$$

In addition to the wind effects, the numeric simulator includes the servo dynamics which are typically represented by a first-order filter [14]. Therefore, the servo outputs $\bar{T}_M$, $\bar{T}_T$ of the main and tail rotor are given by

$$\tau_s\dot{\bar{T}}_M = -\bar{T}_M + T_M \quad \tau_s\dot{\bar{T}}_T = -\bar{T}_T + T_T$$

where τ_s is the rotors time constant. The applied flapping angles $\bar{a}, \bar{b}$ are produced by the flapping dynamics model established in [12], [14], namely

$$\tau_f\dot{\bar{a}} = -\tau_f\omega_y - \bar{a} + a \quad \tau_f\dot{\bar{b}} = -\tau_f\omega_x - \bar{b} + b$$

where τ_f is the main rotor's dynamics time constant. The flapping angles a, b are also saturated to ± 0.25 rad, complying with realistic limitations of actual rotor configurations. The nominal helicopter model parameters, used by the controller, are obtained by [21] for the MIT's small scale rotorcraft X-Cell.60 and presented in Table I. The parameters related to the drag forces and moments as well as the servos time constants are given in Table II. The actual helicopter model of the simulator, includes parametric uncertainty that reach a difference of up to 30% with respect to the nominal values used by the controller. All of the above uncertainty injection is necessary for investigating the robust capabilities of the controller under model and parametric uncertainty which occurs in real life applications.

The proposed control scheme can be easily modified in order to include integral components that will attenuate the steady state tracking error, caused by the parametric and model uncertainty. In particular, the nested saturation vector S and the desired angular velocity component $\omega_{z,d}$ (defined in (16) and (17), respectively), can be enhanced with the position and yaw integral error, as follows:

$$S(\eta_p, y_1, y_2) = \Sigma_3(y_2 + \Sigma_2(W_2 y_1 + \Sigma_1(W_1(\eta_p + y_1))))$$
$$\omega_{z,d} = \frac{C_\theta}{C_\phi}\left[\dot{\psi}_d - \frac{S_\phi}{C_\theta}\omega_y - \lambda_\psi e_\psi - \lambda_\eta \eta_\psi\right]$$

where $\dot{\eta}_p = e_p, \dot{\eta}_\psi = e_\psi, \lambda_\eta > 0$ and W_1, W_2 are diagonal matrices of positive gains. In this case, the requirements of Property 3 become, $L_{i,j} \leq M_{i,j}$ for $i, j = 1, 2, 3$ while $M_{j,i} < L_{j+1,i}$ for $j = 1, 2$ and $i = 1, 2, 3$.

The proposed design will be compared with a fundamental controller of four single-input single-output (SISO) PID feedback loops, proposed in [12]. This control scheme is very common start up design point in real life applications, since it does not require knowledge of the helicopter model and the controller gains can be empirically tuned.

Both of the controllers performance, in terms of tracking accuracy and dexterity, was tested by the execution of two different maneuvers. For the first maneuver, the helicopter reaches a set point while its velocity exponentially decreases and its heading remains constant. The desired trajectory for the first maneuver is

$$p_d^I(t) = \begin{pmatrix} 20 - 20e^{-0.25t} \\ -30 + 30e^{-0.25t} \\ -10 + 10e^{-0.45t} \end{pmatrix} \quad \psi_d(t) = 0.$$

The second maneuver is composed of two parts. In the first part the helicopter lifts vertically for 7 s. Then it performs an "8-shaped" curved path while it continues to lift. Throughout the whole maneuver the vertical velocity is exponentially decreasing while the heading remains constant. For the second maneuver, the desired position and heading are

$$p_d^I(t) = (0 \quad 0 \quad -7(1 - e^{-0.3t}))^T \quad \text{for } t \leq 7$$
$$p_d^I(t) = \begin{pmatrix} 20\left(1 - \cos\frac{2\pi}{23}(t-7)\right) \\ 10\sin\left(\frac{4\pi}{23}(t-7)\right) \\ -7(1 - e^{-0.3t}) \end{pmatrix} \quad \text{for } t > 7$$
$$\psi_d = 0.$$

During the execution of both of the maneuvers, the components of the wind speed in the inertia coordinates are (in m/s)

$$v_w^I(t) = 2\sin(t) \quad v_w^I(t) = 2\cos(0.75t + \pi/2) \quad v_w^I(t) = 0.$$

TABLE I
HELICOPTER PARAMETERS

$\mathcal{I} = diag(0.18, 0.34, 0.28)\ kg \cdot m^2,\ m = 8.2\ kg,\ g = 9.81\ m/sec^2$
$x_t = -0.91\ m,\ z_t = -0.08\ m,\ z_m = -0.235\ m,\ x_m = y_m = y_t = 0$
$c_m = 52\ N \cdot m/rad,\ C^M = 0.004452\ m/\sqrt{N},\ D^M = 0.6304\ N \cdot m$

TABLE II
DRAG AND SERVO PARAMETERS

$d_x^f = 0.06, d_y^f = 0.132, d_z^f = 0.09, d_y^{vf} = 0.0072, d_z^{hs} = 0.006\ kg/m,$
$x_{hs} = -0.71\ m, Vi = 4.2\ m/sec, \tau_s = 0.1\ sec, \tau_f = 0.1\ sec$

TABLE III
CONTROLLER GAINS

$M_{3,i}$	22	Λ_1	diag(3.1,3.1)
$L_{3,i}$	21.5	Λ_2	diag(6,6,3)
$M_{2,i}$	7	W_1	diag(8,8,8)
$L_{2,i}$	6.5	W_2	diag(0.1,0.1,0.1)
$M_{1,i}$	2	λ_ψ	2
$L_{1,i}$	1.5	λ_η	2
for $i = 1, 2, 3$		k	0.1

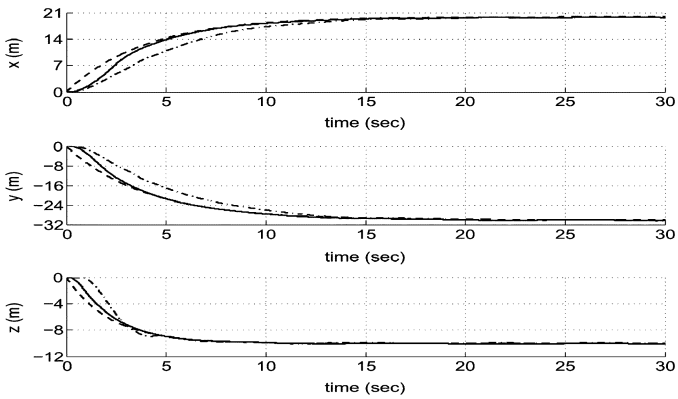

Fig. 2. *First maneuver*: Reference trajectory (dashed line), actual position trajectory of the backstepping (solid line), and PID (dashed-dotted line) designs, expressed in the inertia coordinates, with respect to time.

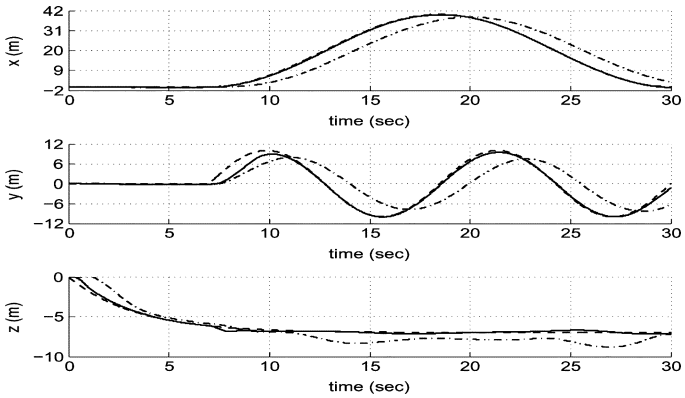

Fig. 3. *Second maneuver*: Reference trajectory (dashed line), actual position trajectory of the backstepping (solid line), and PID (dashed-dotted line) designs, expressed in the inertia coordinates, with respect to time.

The controller gains associated with the attitude dynamics are tuned based on the gain requirements of Theorem 1. They are sufficiently high in order for the helicopter to rapidly obtain its desired orientation. The saturation gains are tuned based on the gain requirements of Property 3. In addition, $\ddot{p}^I_{d,z}$ and $M_{3,3}$ comply with Property 1. To compensate the effect of the anti-torque Q_M and the model uncertainty, a steady state value of the flapping angles is required. This steady state value, through the parasitic forces X_M, Y_M, and Y_T causes an offset in the translational position error. This steady state offset is minimized by increasing the gains of the diagonal matrices W_1, W_2. The controller gains used for the simulation are shown in Table III.

The position response (for both controllers) in the inertia coordinates, versus the desired trajectories with respect to time, are illustrated in Figs. 2 and 3 for the two maneuvers. The helicopter position in inertia coordinates is illustrated in Figs. 4 and 5. The

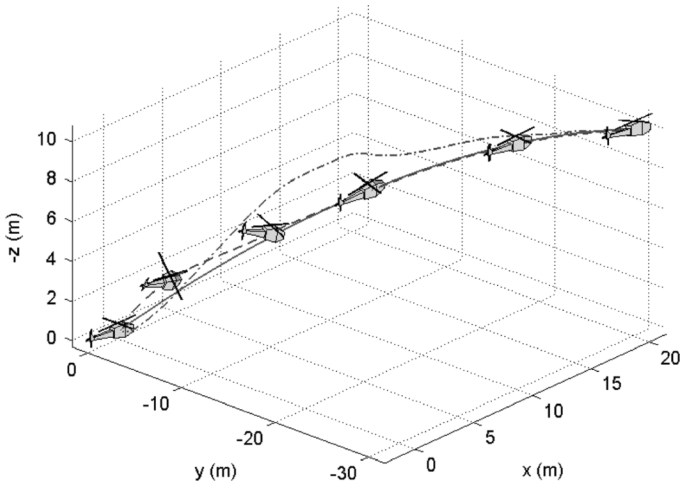

Fig. 4. *First maneuver*: Reference position trajectory (solid line) and the actual trajectory of the backstepping (dashed line), and PID (dashed-dotted line) designs, with respect to the inertia axis.

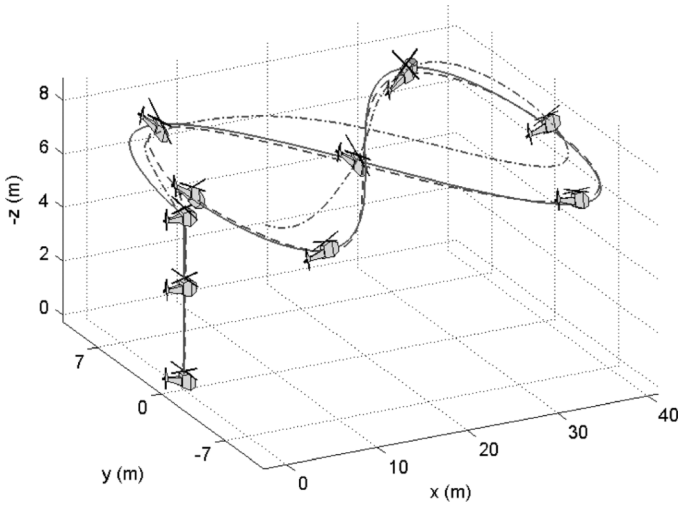

Fig. 5. *Second maneuver*: Reference position trajectory (solid line) and the actual trajectory of the backstepping (dashed line) and PID (dashed-dotted line) designs, with respect to the inertia axis.

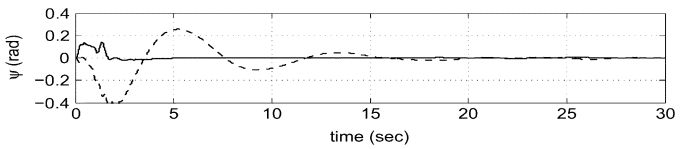

Fig. 6. *First maneuver*: Yaw angle of the backstepping (solid line) and PID (dashed line) designs.

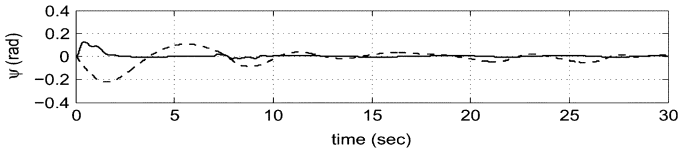

Fig. 7. *Second maneuver*: Yaw angle of the backstepping (solid line) and PID (dashed line) designs.

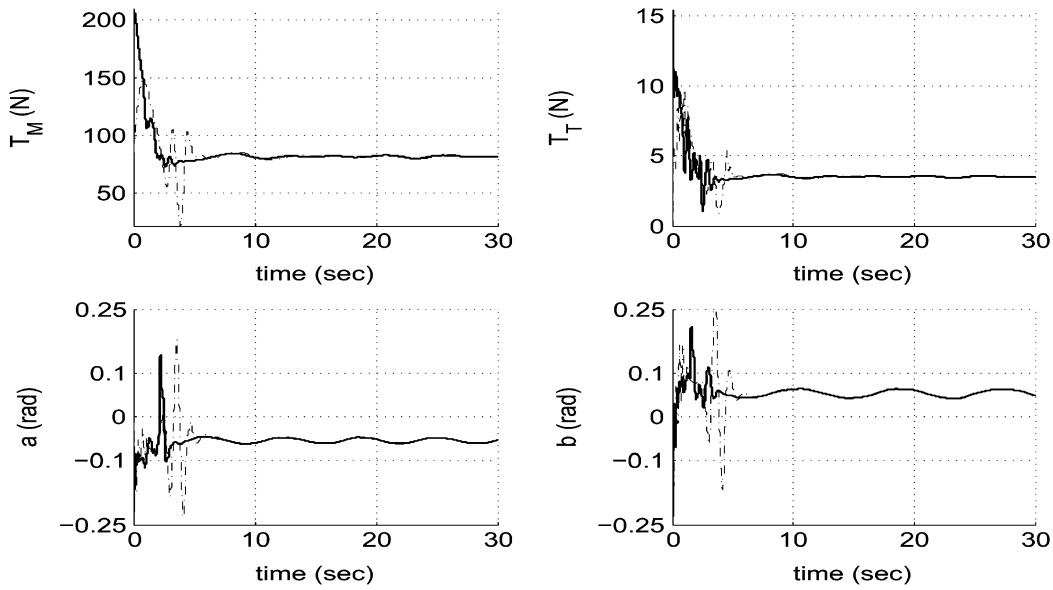

Fig. 8. *First maneuver*: Main and tail rotor thrust T_M, T_T and the flapping angles a, b of the backstepping (solid line) and PID (dashed line) designs.

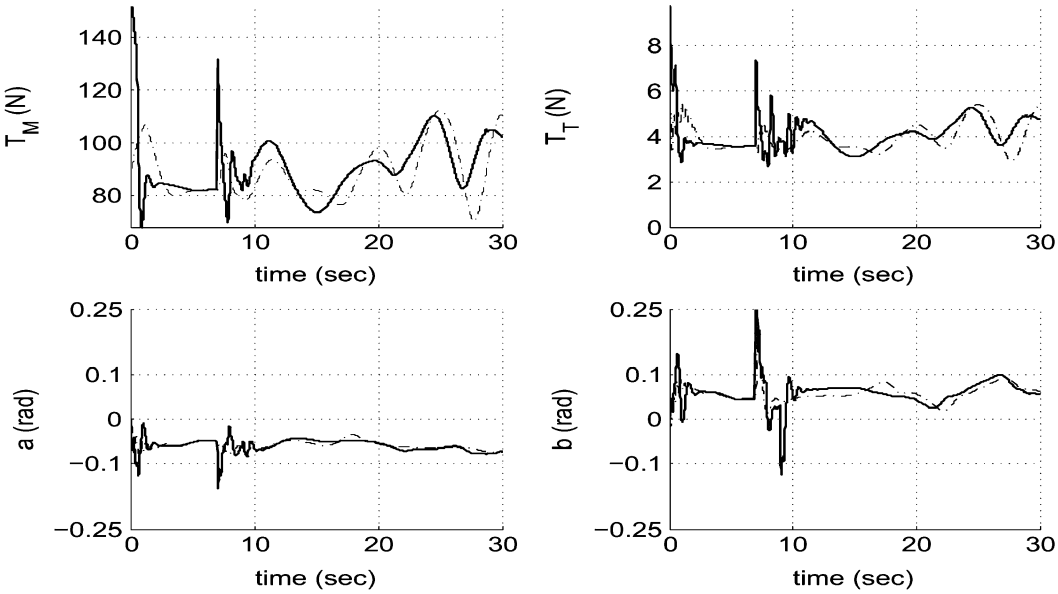

Fig. 9. *Second maneuver*: Main and tail rotor thrust T_M, T_T and the flapping angles a, b of the backstepping (solid line) and PID (dashed line) designs.

heading, for the two control schemes, is depicted in Figs. 6 and 7. Finally, the rotors thrusts and the flapping angles can be seen in Figs. 8 and 9. The numerical results illustrate the controller's successful tracking performance and its advanced tracking capabilities over the PID design. Even though, the proposed design is a model based controller, it exhibits significant robustness attributes towards considerable parametric and model uncertainty.

VIII. Conclusion

This brief has presented a backstepping control design for helicopters. The controller assumes full availability of all the helicopter's state variables of the translational and attitude dynamics. In real life applications the state vector can be obtained by appropriate fusion and filtering of common sensors such as a global positioning system, an inertia measurement unit, accelerometer, and a magnetic compass.

The main idea of the design is the use of the direction and magnitude of the thrust vector to stabilize the position error dynamics. The attitude control design is based on the structural properties of the rotation matrix and it is enhanced with special terms that can guarantee that the helicopter will not overturn in its effort to track the predefined position reference trajectory. The attitude error dynamics will be rendered exponentially stable driving the translational error dynamics globally uniformly asymptotically stable.

References

[1] I. Raptis, K. Valavanis, and W. Moreno, "Nonlinear backstepping control design for miniature helicopters using the rotation matrix," in *Proc. 17th Med. Conf. Control Autom.*, 2009, pp. 1227–1232.

[2] D. Shim, H. Kim, and S. Sastry, "Control system design for rotorcraft-based unmanned aerial vehicles using time-domain system identification," in *Proc. IEEE Int. Conf. Control Appl.*, 2000, pp. 808–813.
[3] J. Gadewadikar, F. Lewis, K. Subbarao, K. Peng, and B. Chen, "H-infinity static output-feedback control for rotorcraft," presented at the AIAA Guid., Nav., Control Conf. Exhibit, Keystone, CO, 2006.
[4] M. La Civita, G. Papageorgiou, W. Messner, and T. Kanade, "Integrated modeling and robust control for full-envelope flight of robotic helicopters," in *Proc. IEEE Int. Conf. Robot. Autom.*, 2003, pp. 552–557.
[5] T. Koo and S. Sastry, "Output tracking control design of a helicopter model based on approximate linearization," in *Proc. 37th IEEE Conf. Decision Control*, 1998, vol. 4, pp. 3635–3640.
[6] E. Frazzoli, M. Dahleh, and E. Feron, "Trajectory tracking control design for autonomous helicopters using a backstepping algorithm," in *Proc. Amer. Control Conf.*, 2000, vol. 6, pp. 4102–4107.
[7] A. Isidori, L. Marconi, and A. Serrani, "Robust nonlinear motion control of a helicopter," *IEEE Trans. Autom. Control*, vol. 48, no. 3, pp. 413–426, Mar. 2003.
[8] L. Marconi and R. Naldi, "Robust full degree-of-freedom tracking control of a helicopter," *Automatica*, vol. 43, pp. 1909–1920, 2007.
[9] R. Mahony and T. Hamel, "Robust trajectory tracking for a scale model autonomous helicopter," *Int. J. Robust Nonlinear Control*, vol. 14, no. 12, pp. 1035–1059, 2004.
[10] P. Castillo, R. Lozano, and A. Dzul, *Modelling and Control of Mini-Flying Machines*. New York: Springer-Verlag, 2005.
[11] E. Lee, H. Shim, L. Park, and K. Lee, "Design of hovering attitude controller for a model helicopter," in *Proc. Soc. Instrument Control Eng.*, 1993, pp. 1385–1390.
[12] B. Mettler, *Identification Modeling and Characteristics of Miniature Rotorcraft*. Norwell, MA: Kluwer, 2003.
[13] W. Johnson, *Helicopter Theory*. Princeton, NJ: Princeton University Press, 1980.
[14] V. Gavrilets, B. Mettler, and E. Feron, "Nonlinear model for a small-size acrobatic helicopter," presented at the AIAA Guid., Nav., Control Conf. Exhibit, Montreal, QC, Canada, 2001.
[15] A. Teel, "Global stabilization and restricted tracking for multiple integrators with bounded controls," *Syst. Control Lett.*, vol. 18, pp. 165–171, 1992.
[16] M. Bejar, A. Isidori, L. Marconi, and R. Naldi, "Robust vertical/lateral/longitudinal control of an helicopter with constant yaw-attitude," presented at the 44th IEEE Conf. Dec. Control, Eur. Control Conf. (CDC-ECC), Seville, Spain, 2005.
[17] I. Raptis, "Linear and nonlinear control of unmaned rotorcraft," Ph.D. dissertation, Dept. Elect. Eng., Univ. South Florida, Tampa, 2010.
[18] A. Loria and E. Panteley, *Advanced Topics in Control Systems Theory: Lecture Notes From FAP 2004*. New York: Springer-Verlag, 2005, ch. 2, pp. 23–64.
[19] A. Teel, "Using saturation to stabilize a class of single-input partially linear composite systems," in *Proc. IFAC NOLCOS Symp.*, 1992, pp. 379–384.
[20] E. Sontag, "Remarks on stabilization and input-to-state stability," in *Proc. 28th IEEE Conf. Dec. Control*, 1989, vol. 2, pp. 1376–1378.
[21] V. Gavrilets, B. Mettler, and E. Feron, "Dynamical model for a miniature aerobatic helicopter," Massachussetts Inst. Technol., Boston, 2001.